

Crystal Structures and ^{77}Se NMR Spectra of Molybdenum(IV) Areneselenolates Having Intramolecular $\text{NH}\cdots\text{Se}$ Hydrogen Bonds

Taka-aki Okamura,^{*,†} Kaku Taniuchi,[†] Keonil Lee,[†] Hitoshi Yamamoto,[†] Norikazu Ueyama,^{*,†} and Akira Nakamura[‡]

Department of Macromolecular Science, Graduate School of Science, Osaka University, Toyonaka, Osaka 560-0043, Japan, and OM Research, 7-2-1308, Minami Ogimachi, Kita-ku, Osaka 530-0052, Japan

Received June 23, 2006

Salts of the monooxomolybdenum(IV,V) areneselenolates having intramolecular $\text{NH}\cdots\text{Se}$ hydrogen bonds, $[\text{Mo}^{\text{IV}}\text{O}(\text{Se}-2\text{-RCONHC}_6\text{H}_4)_4]^{2-}$ ($\text{R} = t\text{-Bu, CH}_3, \text{CF}_3$) and $[\text{Mo}^{\text{VO}}(\text{Se}-2-t\text{-BuCONHC}_6\text{H}_4)_4]^-$, were synthesized and characterized by ^1H nuclear magnetic resonance (NMR), ^{77}Se NMR, electron spin resonance (ESR), UV–visible spectra, X-ray analysis, and electrochemical measurements. ^{77}Se – ^1H correlated spectroscopy (COSY) indicated a significant correlation between amide ^1H and selenolate ^{77}Se atoms through an $\text{NH}\cdots\text{Se}$ hydrogen bond with $^1J(^{77}\text{Se}-^1\text{H}) = 5.4$ Hz coupling. The hydrogen bonds contribute to the positive shift in the Mo(V)/Mo(IV) redox potential. In the crystal structure of $(\text{PPh}_4)_2[\text{Mo}^{\text{IV}}\text{O}(\text{Se}-2\text{-CH}_3\text{CONHC}_6\text{H}_4)_4]$, an $\text{NH}\cdots\text{O}=\text{Mo}$ hydrogen bond was found. Ab initio calculations support the presence of intramolecular $\text{NH}\cdots\text{O}=\text{Mo}$ and $\text{NH}\cdots\text{Se}$ hydrogen bonds.

Introduction

Molybdenum enzymes, with the exception of nitrogenase, are widely distributed in both eukaryotes and prokaryotes. They are known to catalyze the reduction and oxidation of many substrates, and their active sites contain molybdenum–thiolate bonds.¹ One of these enzymes, formate dehydrogenase H, has an additional molybdenum–selenolate (selenocysteine) bond, which is essential for catalytic activity^{2,3} and has been established by X-ray crystallography.⁴ The presence of a hydrogen bond was proposed between selenocysteine and the side chain of a histidine residue and has been believed to play a role in proton-transfer reactions.

Substituting a sulfur atom with selenium is a powerful technique for determining metalloprotein coordination or binding using X-ray absorption, ESR, NMR, and other various spectroscopies.^{5,6} Selenium contains six stable iso-

topes and one of them, ^{77}Se , exhibits $I = 1/2$ and enough natural abundance (7.6%) to use for NMR measurements without any enrichment.⁷

We have systematically investigated the function of $\text{NH}\cdots\text{S}$ hydrogen bonds in metalloproteins (e.g., molybdoenzyme,^{8,9} rubredoxin,^{10,11} ferredoxins,¹² P-450,^{13,14} and copper protein¹⁵) using a variety of model compounds. The presence of $\text{NH}\cdots\text{S}$ hydrogen bonds was established by IR and ^1H NMR spectroscopy. These methods also indicate the

* To whom correspondence should be addressed. E-mail: tokamura@chem.sci.osaka-u.ac.jp (T.O.), ueyama@chem.sci.osaka-u.ac.jp (N.U.).

[†] Osaka University.

[‡] OM Research.

- (1) Hille, R. *Chem. Rev.* **1996**, *96*, 2757–2816.
- (2) Gladyshev, V. N.; Khangulov, S. V.; Axley, M. J.; Stadtman, T. C. *Proc. Natl. Acad. Sci. U.S.A.* **1994**, *91*, 7708–7711.
- (3) Khangulov, S. V.; Gladyshev, V. N.; Dismukes, G. C.; Stadtman, T. C. *Biochemistry* **1998**, *37*, 3518–3528.
- (4) Boyington, J. C.; Gladyshev, V. N.; Khangulov, S. V.; Sun, P. D. *Science* **1997**, *275*, 1305–1308.

- (5) Ralle, M.; Berry, S. M.; Nilges, M. J.; Gieselman, M. D.; van der Donk, W. A.; Lu, Y.; Blackburn, N. J. *J. Am. Chem. Soc.* **2004**, *126*, 7244–7256.
- (6) Johansson, L.; Gafvelin, G.; Arnér, E. S. J. *Biochim. Biophys. Acta* **2005**, *1726*, 1–13.
- (7) Emsley, J. *The Elements*; Oxford Press: Oxford, U.K., 1989.
- (8) Ueyama, N.; Okamura, T.; Nakamura, A. *J. Am. Chem. Soc.* **1992**, *114*, 8129–8137.
- (9) Baba, K.; Okamura, T.; Suzuki, C.; Yamamoto, H.; Yamamoto, T.; Ohama, M.; Ueyama, N. *Inorg. Chem.* **2006**, *45*, 894–901.
- (10) Okamura, T.; Takamizawa, S.; Ueyama, N.; Nakamura, A. *Inorg. Chem.* **1998**, *37*, 18–28.
- (11) Ueyama, N.; Okamura, T.; Nakamura, A. *J. Chem. Soc., Chem. Commun.* **1992**, 1019–1020.
- (12) Ueyama, N.; Yamada, Y.; Okamura, T.; Kimura, S.; Nakamura, A. *Inorg. Chem.* **1996**, *35*, 6473–6484.
- (13) Ueyama, N.; Nishikawa, N.; Yamada, Y.; Okamura, T.; Oka, S.; Sakurai, H.; Nakamura, A. *Inorg. Chem.* **1998**, *37*, 2415–2421.
- (14) Ueyama, N.; Nishikawa, N.; Yamada, Y.; Okamura, T.; Nakamura, A. *J. Am. Chem. Soc.* **1996**, *118*, 12826–12827.
- (15) Okamura, T.; Ueyama, N.; Nakamura, A.; Ainscough, E. W.; Brodie, A. M.; Waters, J. M. *J. Chem. Soc., Chem. Commun.* **1993**, 1658–1659.

strength of the NH bonds and the electron density or negativity of the hydrogen atom. The strength of the hydrogen bond was indirectly estimated from these data. We have previously reported molybdenum arenethiolates having intramolecular NH...S hydrogen bonds, $[\text{Mo}^{\text{IV}}\text{O}(\text{S}-2\text{-RCONHC}_6\text{H}_4)_4]^{2-}$ and $[\text{Mo}^{\text{V}}\text{O}(\text{S}-2\text{-RCONHC}_6\text{H}_4)_4]^-$ (R = CH₃, *t*-Bu, CF₃), and have demonstrated the contribution of the hydrogen bonds to the positive shift of the redox potential.⁸ In this Study, molybdenum areneseelenolates having intramolecular NH...Se hydrogen bonds were synthesized, and the hydrogen bonds were detected directly by ⁷⁷Se-¹H nuclear spin-spin coupling. Although no example of monooxomolybdenum(IV) areneseelenolate has ever been isolated, the NH...Se hydrogen bond facilitated the isolation of the complexes in the reduced state.

Experimental Section

For the molybdenum compounds, all procedures including synthesis, preparation of samples, and spectroscopic measurements were performed under argon atmosphere by the Schlenk technique. The isolated mercury complex is air-stable but the synthesis was carried out in argon atmosphere. The syntheses of the ligands were carried out in air. All solvents were dried and distilled under argon before use. Bis(2-aminophenyl) diselenide,¹⁶ bis(2-acetylaminophenyl) diselenide,¹⁶ $[\text{Mo}^{\text{V}}\text{O}(\text{SPh})_4]^-$ (NEt₄⁺ and PPh₄⁺ salts),¹⁷ $(\text{PPh}_4)_2\text{[Mo}^{\text{IV}}\text{O}(\text{S}-4\text{-ClC}_6\text{H}_4)_4]$,¹⁸ and $(\text{NEt}_4)_2[\text{Mo}^{\text{V}}\text{O}(\text{SePh})_4]$ ¹⁹ were synthesized by the reported methods.

Bis(2-pivaloylaminophenyl) Diselenide. To a CH₂Cl₂ solution (10 mL) of bis(2-aminophenyl) diselenide (1.0 g, 3.0 mmol) containing pyridine (1 mL) was added slowly pivaloyl chloride (3.0 mL, 24 mmol) at room temperature. After stirring with refluxing for 3 h, the solution was concentrated under reduced pressure. The residue was dissolved in diethyl ether and was washed with water, 2% HCl aq, water, 4% NaHCO₃ aq, and water, successively. The organic layer was dried over sodium sulfate and was concentrated under reduced pressure to give orange oil. The material was recrystallized from hot *n*-hexane, and orange needles were obtained. Yield, 1.2 g (83%). ¹H NMR (acetonitrile-*d*₃) δ 8.26 (s, 2H), 7.53 (d, 2H), 7.55 (d, 2H), 7.30 (t, 2H), 7.01 (t, 2H), 1.17 (s, 18H). Anal. Calcd for C₂₂H₂₈N₂O₅Se₂: C, 51.77; H, 5.53; N, 5.53. Found: C, 51.53; H, 5.45; N, 5.38.

Bis(2-trifluoroacetylaminophenyl) Diselenide. To a tetrahydrofuran (THF) (10 mL) solution of bis(2-aminophenyl) diselenide (0.5 g, 1.5 mmol) was added dropwise trifluoroacetic anhydride (0.8 mL, 0.6 mmol) with cooling in an ice bath. The solution was stirred overnight. After removal of solvents, water was added to the residue. The precipitate was washed with water, 2% HCl aq, water, 4% NaHCO₃ aq, and water, successively. The crude product was recrystallized from ethanol to give a yellowish white powder. Yield 0.67 g (86%). ¹H NMR (chloroform-*d*) δ 8.76 (s, 2H), 8.35 (d, 2H), 7.46 (m, 4H), 7.09 (t, 2H).

(PPh₄)[Mo^VO(SePh)₄]. The complex was synthesized by a similar method reported for (NEt₄)[Mo^VO(SePh)₄].¹⁹ Dark-blue powder was obtained and was found pure without recrystallization.

Anal. Calcd for C₄₈H₄₀OPSe₄Mo: C, 53.60; H, 3.75. Found: C, 53.17; H, 4.03.

(PPh₄)[Mo^VO(Se-2-*t*-BuCONHC₆H₄)₄] (1b). The complex was prepared by a ligand exchange method. A mixture of (Ph₄P)[Mo^VO(SePh)₄] (40 mg, 0.05 mmol) and bis(2-pivaloylaminophenyl) diselenide (70 mg, 0.14 mmol) in 1,2-dimethoxyethane (DME, 2 mL) was stirred at room temperature overnight. The precipitate was collected by filtration and was washed with diethyl ether. The blue crude product was recrystallized from hot acetonitrile, and dark blue microcrystals were obtained. Yield 20 mg (30%). Anal. Calcd for C₆₈H₇₆N₄O₅PSe₄Mo: C, 55.48; H, 5.20; N, 3.81. Found: C, 54.05; H, 5.16; N, 3.74. The disagreements of the elemental analyses for **1b** and **1a** are probably caused by their hygroscopic character and the instability of these Mo(V) compounds. The calculated values for **1b**·(H₂O)₂: C, 54.15; H, 5.35; N, 3.72, agree with the found ones.

(NEt₄)[Mo^VO(Se-2-*t*-BuCONHC₆H₄)₄] (1a). The complex was synthesized by a similar method as described for the synthesis of (Ph₄P)[Mo^VO(Se-2-*t*-BuCONHC₆H₄)₄] using (NEt₄)[Mo^VO(SePh)₄]. Dark blue microcrystals were obtained from hot acetonitrile. Anal. Calcd for C₅₂H₇₆N₅O₅Se₄Mo: C, 49.45; H, 6.07; N, 5.55. Calcd for **1a**·(H₂O)₃: C, 47.42; H, 6.28; N, 5.32. Found: C, 47.54; H, 5.89; N, 5.02.

(NEt₄)₂[Mo^{IV}O(Se-2-*t*-BuCONHC₆H₄)₄] (2a). A mixture of (NEt₄)[Mo^VO(SePh)₄] (220 mg, 0.25 mmol) and bis(2-pivaloylaminophenyl) diselenide (460 mg, 0.90 mmol) in DME (10 mL) was stirred at room temperature overnight. The precipitate was collected by filtration and was washed with DME and diethyl ether. After drying under reduced pressure, tetraethylammonium borohydride (37 mg, 0.26 mmol) was added, and the mixture was stirred overnight in DME (10 mL) at room temperature. The precipitate was collected by filtration and was washed with DME until the washings were colorless. The crude powder was dissolved in 20 mL of acetonitrile and was filtered to remove insoluble materials. The solution was concentrated under reduced pressure and the residue was recrystallized from hot acetonitrile/diethyl ether to give purple-red microcrystals. Yield 50 mg (14%). ¹H NMR (acetonitrile-*d*₃) δ 9.08 (s, 4H), 8.11 (d, 4H), 7.56 (d, 4H), 6.98 (t, 4H), 6.68 (t, 4H), 3.08 (q, 16H), 1.21 (s, 36H), 1.15 (t, 24H). Anal. Calcd for C₆₀H₉₆N₆O₅Se₄Mo: C, 51.73; H, 6.95; N, 6.03. Found: C, 51.26; H, 6.88; N, 6.00.

(NEt₄)₂[Mo^{IV}O(Se-2-CH₃CONHC₆H₄)₄] (3a). The complex was synthesized by the same method as described for the synthesis of (NEt₄)₂[Mo^{IV}O(Se-2-*t*-BuCONHC₆H₄)₄] using bis(2-acetylaminophenyl) diselenide. The purple-red microcrystals were obtained in a very low yield (ca. 10%). ¹H NMR (acetonitrile-*d*₃) δ 9.19 (s, 4H), 8.10 (d, 4H), 7.45 (d, 4H), 7.05 (t, 4H), 6.73 (t, 4H), 3.11 (q, 16H), 2.04 (s, 12H), 1.18 (t, 24H). Anal. Calcd for C₄₈H₇₂N₆O₅Se₄Mo: C, 47.07; H, 5.92; N, 6.86. Calcd for **3a**·(H₂O)_{1.5}: C, 46.05; H, 6.04; N, 6.71. Found: C, 45.98; H, 5.88; N, 6.81.

(PPh₄)₂[Mo^{IV}O(Se-2-CH₃CONHC₆H₄)₄] (3b). To a solution of (NEt₄)₂[Mo^{IV}O(Se-2-CH₃CONHC₆H₄)₄] (9.1 mg, 7.9 × 10⁻⁶ mol) in acetonitrile was added an acetonitrile solution (1 mL) of Ph₄PBr (7.5 mg, 1.8 × 10⁻⁵ mol). Dark reddish-purple crystals were deposited, which were washed with acetonitrile. The crystals were recrystallized from hot acetonitrile to give reddish-purple plates. This compound was characterized by X-ray analysis.

(PPh₄)₂[Mo^{IV}O(Se-2-CF₃CONHC₆H₄)₄] (4). A solution of (PPh₄)₂[Mo^{IV}O(S-4-ClC₆H₄)₄] (51 mg, 3.8 × 10⁻⁵ mol) and (Se-*o*-CF₃CONHC₆H₄)₂ (48 mg, 9.0 × 10⁻⁵ mol) in acetonitrile (2 mL) was stirred for 1 day. The solution was concentrated under reduced pressure. Diethyl ether was added to the solution and the mixture was refrigerated to afford red plates, which were washed with

(16) Keimatsu, S.; Satoda, I. *Yakugaku Zasshi* **1936**, *56*, 600–607.

(17) Boyd, I. W.; Dance, I. G.; Murray, K. S.; Wedd, A. G. *Aust. J. Chem.* **1978**, *31*, 279–284.

(18) Kondo, M.; Ueyama, N.; Fukuyama, K.; Nakamura, A. *Bull. Chem. Soc. Jpn* **1993**, *66*, 1391–1396.

(19) Hanson, G. R.; Brunette, A. A.; McDonnell, A. C.; Murray, K. S.; Wedd, A. G. *J. Am. Chem. Soc.* **1981**, *103*, 1953–1959.

diethyl ether and were dried in vacuo. Yield 24 mg (32%). ¹H NMR (acetonitrile-*d*₃) δ 9.83 (s, 4H), 8.05 (d, 4H), 7.6–7.9 (m, 40H), 7.54 (d, 4H), 7.10 (t, 4H), 6.84 (t, 4H). Anal. Calcd for C₈₀H₆₀N₄O₅F₁₂P₂Se₄Mo: C, 51.69; H, 3.25; N, 3.01. Found: C, 51.47; H, 3.12; N, 4.50.

Hg(Se-2-*t*-BuCONHC₆H₄)₂. To a methanol solution (10 mL) of bis(2-pivaloylaminoethyl) diselenide (230 mg, 0.45 mmol) was added sodium borohydride until the solution turned colorless at room temperature. After the solution was stirred for 5 min, acetic acid (4.0 mL) was added to hydrolyze the excess of sodium borohydride. Mercury(II) dichloride (230 mg, 0.85 mmol) was added to the solution which was stirred for 3 h. The clear solution was concentrated under reduced pressure to give orange oil. After addition of saturated NaCl aq (100 mL), the crude product was extracted by diethyl ether (400 mL). The organic layer was separated and washed successively with 2% HCl aq, water, 4% NaHCO₃ aq, water, and sat. NaCl aq. The solution was dried over anhydrous sodium sulfate and was concentrated under reduced pressure. The resulting orange solid was recrystallized from diethyl ether/*n*-hexane to give air-stable colorless needles. Yield 105 mg (33%). ¹H NMR (Me₂SO-*d*₆); δ 8.94(s, 2H), 7.94(d, 2H), 7.66(d, 2H), 7.20(t, 2H), 6.90(t, 2H), 1.23(s, 18H); ¹³C NMR (Me₂SO-*d*₆); δ 175.71, 139.86, 137.63, 127.60, 124.08, 121.67, 120.72, 27.35. Anal. Calcd for C₂₂H₂₈N₂O₂Se₂Hg: C, 37.17; H, 3.97; N, 3.94. Found: C, 37.34; H, 4.04; N, 3.79.

Physical Measurements. Visible spectra in DMF solution were recorded on a Jasco Ubest-30 spectrometer. ¹H NMR spectra were taken on a JEOL GSX-400 spectrophotometer operating at 399.65 MHz. ⁷⁷Se NMR spectra were obtained at room temperature on a 76.10 MHz JEOL GSX 400 spectrometer using dimethyl selenide in DMF-*d*₇ as an external standard of the chemical shift. IR spectra in solid state were recorded on a Jasco FT/IR-3 spectrophotometer. Electrochemical measurements were carried out using a Yanaco P-1100 instrument in DMF that contained 0.1 M tetra-*n*-butylammonium perchlorate as a supporting electrolyte. *E*_{1/2} value, determined as (*E*_{p,a} + *E*_{p,c})/2, was referenced to the saturated calomel electrode (SCE) electrode at room temperature. ESR spectra in acetonitrile/DMF (4/1 v/v) were recorded on a JEOL RE-2X spectrometer at room temperature and at -150 °C.

X-ray Analysis. Each single crystal of (PPh₄)₂[Mo^{IV}O(Se-2-RCONHC₆H₄)₄] (R = CH₃(**3b**), CF₃(**4**)) was mounted in a loop with Nujol, which was frozen immediately in a stream of cold nitrogen at 100 K. Data collections were made on a Rigaku RAXIS-RAPID Imaging Plate diffractometer with graphite monochromated Mo Kα radiation (0.71075 Å). The structures were solved by direct method using SIR92²⁰ and were expanded by Fourier technique using SHELXL-97.²¹ Complex **4** has a crystallographical center of symmetry. All hydrogen atoms were placed at the calculated positions using the riding model. Non-hydrogen atoms were refined anisotropically. The final Fourier map did not show any significant features. The crystallographic data are listed in Table 1.

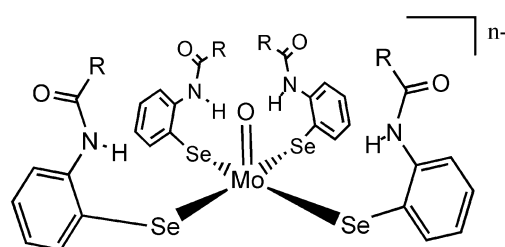
Ab Initio Molecular Orbital Calculations. Single-point MO calculations of the anion part of **3b**, [Mo^{IV}O(Se-2-CH₃-CONHC₆H₄)₄]²⁻, and a pair of the anion and the cation of **4**, [(PPh₄)[Mo^{IV}O(Se-2-CF₃CONHC₆H₄)₄]]⁻, were performed using Gaussian 03²² program package with 3-21G** basis set. The coordinates of the crystal structure were used without any geometrical optimization. The bond orders of hydrogen bonds were

Table 1. Crystallographic Data

	3b	4
chemical formula	C ₈₀ H ₇₂ N ₄ O ₅ P ₂ Se ₄ Mo	C ₈₀ H ₆₀ N ₄ O ₅ F ₁₂ P ₂ Se ₄ Mo
fw	1643.20	1859.09
cryst syst	monoclinic	triclinic
space group	<i>P</i> 2 ₁	<i>P</i> 1̄
<i>a</i> , Å	14.728(15)	12.624(9)
<i>b</i> , Å	13.149(11)	13.420(8)
<i>c</i> , Å	19.335(15)	13.886(9)
α, deg	90	61.934(17)
β, deg	109.61(3)	66.77(2)
γ, deg	90	69.349(18)
<i>V</i> , Å ³	3527(5)	1867(2)
<i>Z</i>	2	1
<i>d</i> _{calc} , g cm ⁻³	1.547	1.654
abs coeff, mm ⁻¹	2.351	2.254
no. of ind refls	11079	8489
<i>R</i> ^a [<i>I</i> > 2σ(<i>I</i>)]	0.0475	0.0429
<i>wR</i> ^b (all data)	0.0668	0.0867

$$^a R1 = \sum ||F_o| - |F_c|| / \sum |F_o|. \quad ^b wR2 = \{ \sum [w(F_o^2 - F_c^2)^2] / \sum [w(F_o^2)^2] \}^{1/2}$$

Chart 1



		NEt ₄ ⁺	PPh ₄ ⁺
<i>n</i> = 1 (Mo ^V)	R = <i>t</i> -Bu	1a	1b
<i>n</i> = 2 (Mo ^{IV})	R = <i>t</i> -Bu	2a	2b
	CH ₃	3a	3b
	CF ₃		4

calculated using the program BORDER²³ on the basis of the wave function obtained in Gaussian calculations.

Results and Discussion

Syntheses. To synthesize the monooxomolybdenum(V) areneselenolate (Chart 1), (NEt₄)[Mo^VO(Se-2-*t*-BuCONHC₆H₄)₄] (**1a**), a similar method as described for (NEt₄)[Mo^VO(S-2-*t*-BuCONHC₆H₄)₄] was used (eq 1).⁸ Subsequent

(20) Altomare, A.; Burla, M. C.; Camalli, M.; Cascarano, M.; Giacovazzo, C.; Guagliardi, A.; Polidori, G. *J. Appl. Crystallogr.* **1994**, *27*, 435.

(21) Sheldrick, G. M. *SHELXL-97—Program for the Refinement of Crystal Structures*; University of Goettingen: Goettingen, Germany, 1997.

(22) Frisch, M. J.; Trucks, G. W.; Schlegel, H. B.; Scuseria, G. E.; Robb, M. A.; Cheeseman, J. R.; Montgomery, J. A., Jr.; Vreven, T.; Kudin, K. N.; Burant, J. C.; Millam, J. M.; Iyengar, S. S.; Tomasi, J.; Barone, V.; Mennucci, B.; Cossi, M.; Scalmani, G.; Rega, N.; Petersson, G. A.; Nakatsuji, H.; Hada, M.; Ehara, M.; Toyota, K.; Fukuda, R.; Hasegawa, J.; Ishida, M.; Nakajima, T.; Honda, Y.; Kitao, O.; Nakai, H.; Klene, M.; Li, X.; Knox, J. E.; Hratchian, H. P.; Cross, J. B.; Bakken, V.; Adamo, C.; Jaramillo, J.; Gomperts, R.; Stratmann, R. E.; Yazyev, O.; Austin, A. J.; Cammi, R.; Pomelli, C.; Ochterski, J. W.; Ayala, P. Y.; Morokuma, K.; Voth, G. A.; Salvador, P.; Dannenberg, J. J.; Zakrzewski, V. G.; Dapprich, S.; Daniels, A. D.; Strain, M. C.; Farkas, O.; Malick, D. K.; Rabuck, A. D.; Raghavachari, K.; Foresman, J. B.; Ortiz, J. V.; Cui, Q.; Baboul, A. G.; Clifford, S.; Cioslowski, J.; Stefanov, B. B.; Liu, G.; Liashenko, A.; Piskorz, P.; Komaromi, I.; Martin, R. L.; Fox, D. J.; Keith, T.; Al-Laham, M. A.; Peng, C. Y.; Nanayakkara, A.; Challacombe, M.; Gill, P. M. W.; Johnson, B.; Chen, W.; Wong, M. W.; Gonzalez, C.; Pople, J. A. *Gaussian 03*, revision B.05; Gaussian, Inc.: Wallingford, CT, 2003.

(23) Mayer, I.; *Program BORDER*, version 1.0; Chemical Research Center, Hungarian Academy of Science: Budapest, Hungary, 2005.

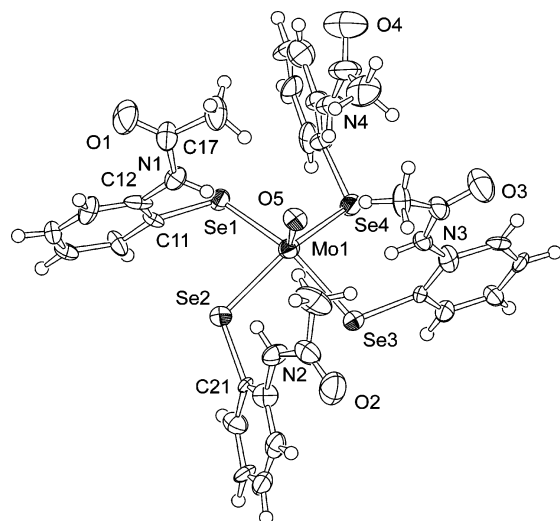
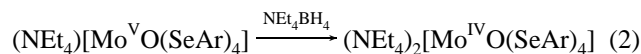
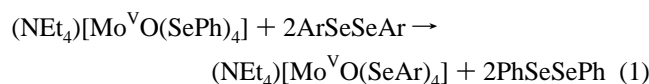
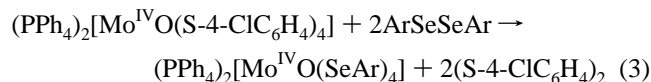


Figure 1. Molecular structure (anion part) of **3b**.

reduction by NEt_4BH_4 produced the corresponding molybdenum(IV) complex (eq 2), where SeAr represents Se-2-RCONHC₆H₄.



When $(\text{NEt}_4)[\text{Mo}^{\text{V}}\text{O}(\text{SPh})_4]$ was used as a starting material, an incomplete ligand-exchange reaction was observed and **1a** could not be isolated; however, $(\text{PPh}_4)[\text{Mo}^{\text{V}}\text{O}(\text{SPh})_4]$ gave $(\text{PPh}_4)[\text{Mo}^{\text{V}}\text{O}(\text{Se}-2-t\text{-BuCONHC}_6\text{H}_4)_4]$ (**1b**) because of the poor solubility and good crystallinity characteristics of the product. In the case of R = CH₃ or CF₃, $(\text{NEt}_4)[\text{Mo}^{\text{V}}\text{O}(\text{Se}-2\text{-RCONHC}_6\text{H}_4)_4]$ could not be isolated and was found to decompose easily during the purification process. $(\text{PPh}_4)_2[\text{Mo}^{\text{IV}}\text{O}(\text{Se}-2\text{-CF}_3\text{CONHC}_6\text{H}_4)_4]$ (**4**) was synthesized successfully from $(\text{PPh}_4)_2[\text{Mo}^{\text{IV}}\text{O}(\text{S}-4\text{-ClC}_6\text{H}_4)_4]$ ¹⁸ and the diselenide of the ligand (eq 3).



Molecular Structure in the Crystal and Conformation in Solution. Crystal structures of **3b** and **4** are shown in Figures 1 and 2, respectively. The selenolate complex **3b** is isomorphous and isostructural to the corresponding thiolate complex $(\text{PPh}_4)_2[\text{Mo}^{\text{IV}}\text{O}(\text{S}-2\text{-CH}_3\text{CONHC}_6\text{H}_4)_4]$ (**5**).⁸ The MoOSe₄ cores of both of these complexes exhibit a square pyramidal structure. The mean Mo–Se bond length (2.524 Å) of **3b** is longer than that of **5** (2.408 Å) by 0.116 Å because of the difference of the atomic radii (ca. 0.1 Å), which is similar to or slightly larger than the reported values (0.107–0.112 Å) for $[\text{M}(\text{QPh})_4]^{2-}$ (M = Zn(II), Cd(II),²⁴ Fe(II)^{25,26}). The two diagonal Se–Mo–Se angles are 147.48-

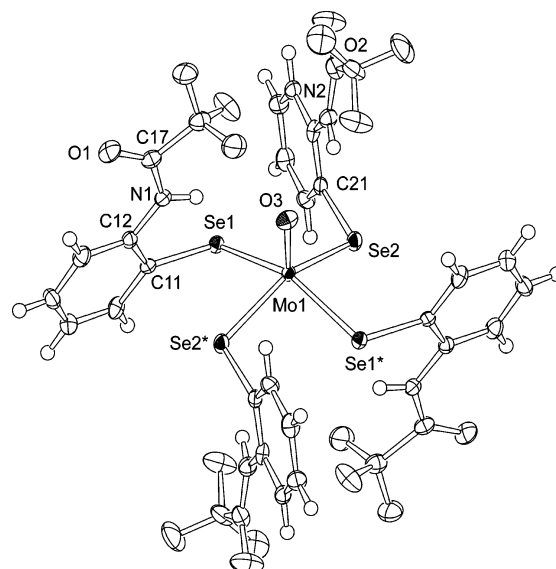


Figure 2. Molecular structure (anion part) of **4**.

(4)° and 143.22(4)° for **3b** and 151.61(4)° and 151.04(4)° for **4**. The differences between the two Se–Mo–Se angles for each complex are 4.26° and 0.57°, respectively, which indicate that each MoOSe₄ core has a typical square-pyramidal geometry. The corresponding thiolate complex **5** has a larger value (7.16°). A geometrical distortion toward a trigonal bipyramidal structure has been known for the molybdenum(V) thiolate $(\text{PPh}_4)[\text{Mo}^{\text{V}}\text{O}(\text{S}-2\text{-CH}_3\text{CONHC}_6\text{H}_4)_4]$ (12.76°).⁸ The geometrical distortion is in agreement with the shortening of the Mo–Q bond length, Mo^V–S (mean 2.397 Å) < Mo^{IV}–S (2.408 Å) < Mo^{IV}–Se (2.524 Å). The mean O–Mo–Q–C (Q = Se or S) torsion angles (–82.5° for **3b**, –85.1° for **4**) are similar to that (81.4°) of **5**. The Mo–Se–C–C torsion angles (mean 68.6°) of **3b** are also similar to the Mo–S–C–C torsion angle (mean –69.8°) of **5**. The large 4pπ orbital of the selenium atom enables the formation of the NH...Se hydrogen bond; however, the direction of the amide NH is not so desirable. Interestingly, one (N1H1) of the four amide NH groups in **3b** is directed to O=Mo rather than to Se, where the torsion angle between the amide plane and the benzene ring, C13–C12–N1–C17, is –43°. This unexpected NH...O=Mo interaction is discussed in a subsequent section using molecular orbital (MO) calculations. The four acylamino groups have been believed to be located predominantly on the same side (all up) as the Mo=O, as illustrated in Chart 1. When the bulky *t*-BuCONH– group was used, a minor conformer with alternatively directed (up–down–up–down) acylamino groups was detected in solution by ¹H NMR. When the crystal structure of **4** was examined, a new conformer (up–up–down–down) was found. This conformation gave an open Mo=O site to allow access of PPh₄⁺ cation to form intermolecular Mo=O...H–C hydrogen bond as shown in Figure S1. The short O...H contact (2.428 Å) shows a

(24) Ueyama, N.; Sugawara, T.; Sasaki, K.; Nakamura, A.; Yamashita, S.; Wakatsuki, Y.; Yamazaki, H.; Yasuoka, N. *Inorg. Chem.* **1988**, *27*, 741–747.

(25) Coucouvanis, D.; Swenson, D.; Baenziger, N. C.; Murphy, C.; Holah, D. G.; Sfaras, N.; Simopoulos, A.; Kostikas, A. *J. Am. Chem. Soc.* **1981**, *103*, 3350–3362.

(26) McConnachie, J. M.; Ibers, J. A. *Inorg. Chem.* **1991**, *30*, 1770–1773.

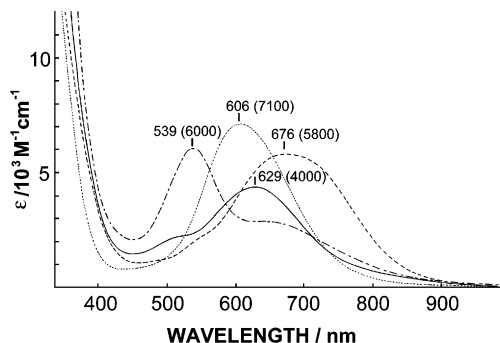


Figure 3. Absorption spectra of **1b** (solid line), $(\text{PPh}_4)[\text{Mo}^{\text{VO}}(\text{SePh})_4]$ (dashed line), $(\text{PPh}_4)[\text{Mo}^{\text{VO}}(\text{S-2-}t\text{-BuCONHC}_6\text{H}_4)_4]$ (dotted-dashed line), and $(\text{PPh}_4)[\text{Mo}^{\text{VO}}(\text{SPh})_4]$ (dotted line) in DMF at room temperature.

bonding character, where the bond order was calculated to be 0.0320 by MO calculations.^{22,23}

In solution, the most stable conformer is different from that in the crystal. ¹H NMR spectra of **4** in acetonitrile-*d*₃ showed one set of signals for the coordinated ligand, indicating that only one conformer was present in solution. The pseudosymmetrical center of the asymmetric compound **4** and the intermolecular attractive Mo=O⋯H–C interaction are presumably favorable for packing. When the complex is dissolved in acetonitrile, the formation of intramolecular hydrogen bonds and the electrostatic interactions between acylamino and Mo=O moieties⁸ dominate the conformation, resulting in an all-up structure. If bulky *t*-BuCONH– groups were introduced to the complex, a minor conformer was detected, as shown in Figure S2. At the higher temperature, the minor conformer increased. The content of the minor conformer at 30 °C is 6% which is smaller than that for the corresponding thiolate (20%).⁸ The calculated thermodynamic parameters for this equilibrium, ΔH and ΔS , are 54 kJ mol^{–1} and 150 J K^{–1} mol^{–1}, respectively. The longer Mo–Se bonds reduce the steric congestion of the bulky *t*-Bu groups. The ESR spectrum of **1b** in a mixture of acetonitrile and DMF at room temperature did not show the presence of the minor conformer as described in a subsequent section.

Absorption Spectra. Monooxomolybdenum(V) arenethiolate and selenolate complexes exhibit characteristic ligand-to-metal charge transfer (LMCT) bands in the visible region.¹⁹ Figure 3 shows absorption spectra of **1b**, $(\text{PPh}_4)[\text{Mo}^{\text{VO}}(\text{SePh})_4]$, $(\text{PPh}_4)[\text{Mo}^{\text{VO}}(\text{S-2-}t\text{-BuCONHC}_6\text{H}_4)_4]$, and $(\text{PPh}_4)[\text{Mo}^{\text{VO}}(\text{SPh})_4]$ in DMF. Substituting S with Se displaces the LMCT band to lower energy, as reported for $[\text{Mo}^{\text{VO}}(\text{QPh})_4]^-$ (Q = Se, S).¹⁹ In the case of $(\text{Ph}_4\text{P})[\text{Mo}^{\text{VO}}(\text{Q-2-}t\text{-BuCONHC}_6\text{H}_4)_4]$ (Q = Se, S), a similar trend was observed, except for splitting of the LMCT peak. In the thiolate complex, splitting of an absorption band was observed, which has been considered to be caused by geometrical distortion from a square pyramidal to a trigonal bipyramidal structure.⁸ The spectrum of **1b** did not exhibit such splitting, which suggests that the MoOSe₄ core has a symmetrical square pyramidal geometry and that the four Mo–Se bonds are equivalent.

ESR Spectra. As shown in Table 2, the ESR spectrum of **1b** ($g_{\parallel} = 2.073$, $g_{\perp} = 2.001$, $A_{\parallel} = 51.1 \times 10^{-4} \text{ cm}^{-1}$, $A_{\perp} =$

Table 2. ESR Parameters for Mo(V) Complexes^a

compounds	g_{iso}	g_{\parallel}	g_{\perp}	A_{iso}^e	A_{\parallel}^e	A_{\perp}^e
$(\text{PPh}_4)[\text{Mo}^{\text{VO}}(\text{Se-2-}t\text{-BuCONHC}_6\text{H}_4)_4]$ (1b) ^b	2.022	2.073	2.001	32.4	51.1	21.9
$(\text{NEt}_4)[\text{Mo}^{\text{VO}}(\text{SePh})_4]^c$	2.024	2.072	2.005	30.0	48.3	21.2
$(\text{NEt}_4)[\text{Mo}^{\text{VO}}(\text{S-2-}t\text{-BuCONHC}_6\text{H}_4)_4]^d$	1.994	2.035	1.981	33.2	54.9	23.4
$(\text{NEt}_4)[\text{Mo}^{\text{VO}}(\text{SPh})_4]^e$	1.990	2.019	1.979	32.3	52.3	22.3

^a Conditions: 1 mM in acetonitrile/DMF (=4:1 v/v) at 77 K and room temperature. ^b At room temperature and –150 °C. ^c Reference 19. ^d Reference 8. ^e 10^{-4} cm^{-1} .

$21.9 \times 10^{-4} \text{ cm}^{-1}$) at –150 °C is comparable to reported values for $[\text{Mo}^{\text{VO}}(\text{SePh})_4]^-$ determined under similar conditions.¹⁹ In the case of the thiolates, introduction of *t*-BuCONH groups increased g_{\parallel} value by the distortion of Mo^{VO}S₄ core.⁸ Additionally, only one conformational isomer was found at room temperature ($g_{\text{iso}} = 2.022$, $A_{\text{iso}} = 32.4 \times 10^{-4} \text{ cm}^{-1}$) without splitting, whereas the conformational isomers of $(\text{NEt}_4)[\text{Mo}^{\text{VO}}(\text{S-2-}t\text{-BuCONHC}_6\text{H}_4)_4]$ were detected as splitting of peak in the previous study.⁸ In contrast to the Mo–S bond, the Mo–Se bond is longer and its presence results in the elimination of the geometrical distortion. This finding is consistent with the crystal structure of the corresponding Mo(IV) compounds, as described in the previous section.

The one-electron reduction from Mo^V (d¹) to Mo^{IV} (d² low spin) increased the band gap between the filled orbital of the ligand and the vacant orbital of the metal ion, which resulted in a high-energy shift of the LMCT band. $(\text{NEt}_4)_2[\text{Mo}^{\text{VO}}(\text{Se-2-}t\text{-BuCONHC}_6\text{H}_4)_4]$ (**2a**) exhibited LMCT at 300 nm ($25\,000 \text{ M}^{-1} \text{ cm}^{-1}$) and a d–d transition at 590 nm ($300 \text{ M}^{-1} \text{ cm}^{-1}$) in DMF, as shown in Figure S3. The d–d band of the corresponding Mo(V) complex was probably masked by the intense LMCT band in this region. These results are similar to those reported for the analogous thiolate compounds.⁸

IR Spectra. The presence of NH⋯Se hydrogen bonds was established by IR spectra. **1b** and **2a** exhibited $\nu(\text{NH})$ at 3325 and 3290 cm^{–1}, respectively, in the solid state (Figure S4). Reduction of the Mo(V) complex to Mo(IV) resulted in a low wavenumber shift of $\nu(\text{NH})$ by 35 cm^{–1}. In contrast, the $\nu(\text{C=O})$ bands were little affected by this reduction; **1b** and **2a** exhibited $\nu(\text{C=O})$ bands at 1673 and 1670 cm^{–1}, respectively, which are considered normal positions for free $\nu(\text{C=O})$ bands without intermolecular NH⋯O=C hydrogen bonds. The diselenide $(\text{Se-2-}t\text{-BuCONHC}_6\text{H}_4)_2$ exhibited the $\nu(\text{NH})$ band at 3292 cm^{–1} and the $\nu(\text{C=O})$ band at 1650 cm^{–1} in the solid state, suggesting the presence of intermolecular NH⋯O=C hydrogen bonds. Under similar conditions, $\nu(\text{NH})$ bands of $(\text{NEt}_4)[\text{Mo}^{\text{VO}}(\text{S-2-}t\text{-BuCONHC}_6\text{H}_4)_4]$ and $(\text{PPh}_4)_2[\text{Mo}^{\text{VO}}(\text{S-2-CH}_3\text{CONHC}_6\text{H}_4)_4]$ were found at 3330 cm^{–1} and at 3272 cm^{–1}, respectively.⁸ The enhancements of the NH⋯Se and the NH⋯S hydrogen bonds by the reduction of the molybdenum center are explained by the increase of the electron density on selenium and sulfur, which is ascribed to the decrease of the electron donation to the metal ion. Generally, a covalent metal–sulfur bond or a high-valent metal ion results in weak NH⋯S hydrogen

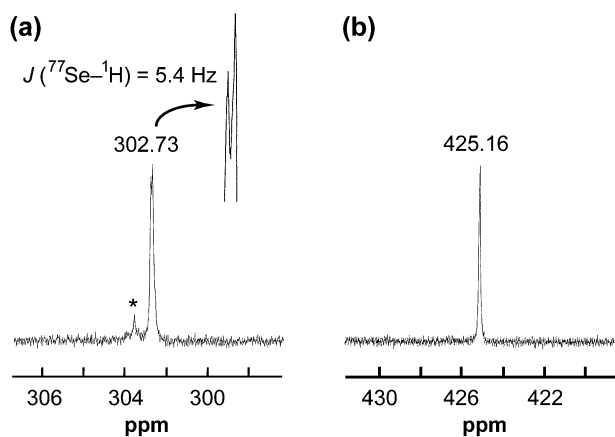


Figure 4. 76.10 MHz ^{77}Se NMR spectra of (a) **2a** and (b) (Se-2-*t*-BuCONHC $_6$ H $_4$) $_2$ in DMF- d_7 at 30 °C. The asterisk denotes a signal of impurity.

bonds, which is caused by the electron donation to electron-deficient metal ion.^{8,27}

Electrochemical Properties. Cyclic voltammograms of **1b** and (PPh $_4$)[MoV(O)(SePh) $_4$] in DMF are shown in Figure S5. Quasi-reversible Mo(IV)/Mo(V) redox couples were found at -0.41 V versus SCE for **1b** and at -0.79 V for the benzeneselenolate.²⁸ Analogous compounds, (PPh $_4$)[MoV(O)(S-2-*t*-BuCONHC $_6$ H $_4$) $_4$] and (PPh $_4$)[MoV(O)(SPh) $_4$], showed similar couples at -0.45 and -0.84 V, respectively, in the same conditions. The NH \cdots Se hydrogen bond positively shifted the redox potential by 0.38 V, which is almost the same as the value (0.39 V) obtained for the effect of the NH \cdots S hydrogen bond.⁸

Detection of NH \cdots Se Hydrogen Bonds by ^{77}Se NMR. ^{77}Se is a stable and NMR-active isotope with $I = 1/2$ and exists 7.6% in natural abundance.⁷ The one-dimensional ^{77}Se NMR spectrum of **2a** showed a doublet at 302.73 ppm from Me $_2$ Se in DMF- d_7 . The splitting indicates that the ^{77}Se - ^1H spin-spin coupling constant $^1J(^{77}\text{Se}-^1\text{H}) = 5.4$ Hz. The 1J constant through the covalent Se-H bond in RSeH has been reported to be 42–43 Hz.²⁹ The ^{77}Se - ^1H spin-spin coupling constant through the NH \cdots Se=C hydrogen bond in selones has been reported as $J_{\text{Se-H}} = \text{ca. } 12\text{--}13$ Hz.³⁰ The relatively small J coupling constant of **2a** indicates weak spin-spin coupling through the hydrogen bond. On the other hand, diselenide (Se-2-*t*-BuCONHC $_6$ H $_4$) $_2$ did not exhibit any splitting of the peak at 425.16 ppm as shown in Figure 4, suggesting that the NH \cdots Se hydrogen bond was absent or too weak to be detected. The covalent Se-Se bond did not cause enough negative charge on the selenium atom to form a hydrogen bond. A similar situation was observed in disulfide, which did not produce any NH \cdots S hydrogen bonds despite a short N \cdots S contact.³¹

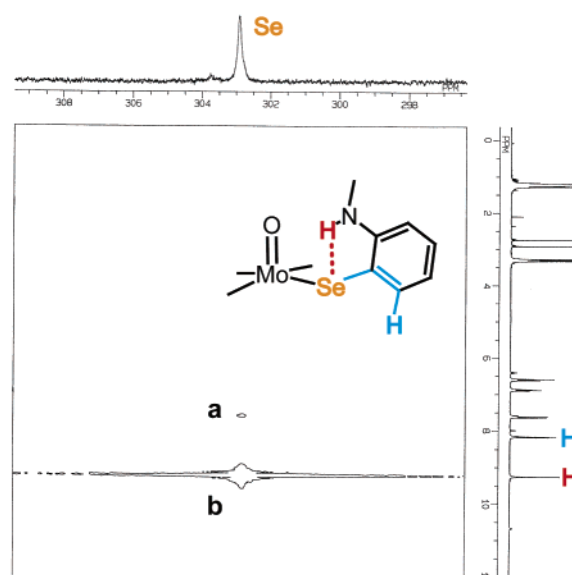


Figure 5. ^{77}Se - ^1H COSY spectrum of **2a** in DMF- d_7 at 30 °C. Two cross-peaks were found, which were assigned to (a) Se and aromatic proton at 2-position through an aromatic ring (blue) and (b) Se and amide NH group through an NH \cdots Se hydrogen bond (red).

The ^{77}Se - ^1H correlated spectroscopy (COSY) clearly indicates that the ^{77}Se - ^1H coupling occurs through the NH \cdots Se hydrogen bond and not via the other pathway. Figure 5 shows the ^{77}Se - ^1H COSY spectrum of **2a** in DMF- d_7 . Two cross-peaks, **a** and **b**, were found. The blue proton in Figure 5 couples with Se via three covalent bonds (H-C-C-Se), including the benzene ring, whereas the red proton couples with Se through NH \cdots Se hydrogen bond. The correlated peak **b** is obviously larger than **a**. This result indicates clearly that the NH \cdots Se hydrogen bond is the predominant pathway for the spin-spin coupling. In the case of a covalent metal-selenolate bond, the hydrogen bond is weaker. Actually, Hg(Se-2-*t*-BuCONHC $_6$ H $_4$) $_2$ exhibited a weak NH \cdots Se hydrogen bond. The IR spectrum of this Hg complex showed the $\nu(\text{NH})$ band at 3341 cm^{-1} in the solid state, which is higher than that of **2a** by 51 cm^{-1} . One-dimensional ^{77}Se NMR did not exhibit any splitting of the signal, as shown in Figure S6a. However, such a weak NH \cdots Se hydrogen bond could be detected by ^{77}Se - ^1H COSY spectra (Figure S6b). The distinct peak clearly indicates the presence of NH \cdots Se hydrogen bonds.

Molecular Orbital (MO) Calculations. As mentioned previously, unexpected NH \cdots O=Mo contact was found in the crystal structure of **3b**. Ball-and-stick representations of **3b** are shown in Figure 6. Three of four amide NH groups were located to form intraligand NH \cdots Se hydrogen bonds. However, one amide (N1-H) group is distinguishable from the other NH groups. Evidently, this amide NH group is directed to the terminal oxo ligand, suggesting the formation of an NH \cdots O=Mo hydrogen bond. In the molybdenum(V) thiolate analogue, all amide NH groups were found to be a good location for forming intramolecular NH \cdots S hydrogen bonds rather than NH \cdots O=Mo hydrogen bonds, and MO calculations showed a weak repulsion between NH and O=Mo moieties.⁸ On the other hand, hydrogen bonds to

(27) Ueyama, N.; Taniuchi, K.; Okamura, T.; Nakamura, A.; Maeda, H.; Emura, S. *Inorg. Chem.* **1996**, *35*, 1945–1951.

(28) Bradbury, J. R.; Masters, A. F.; McDonnell, A. C.; Brunette, A. A.; Bond, A. M.; Wedd, A. G. *J. Am. Chem. Soc.* **1981**, *103*, 1959–1964.

(29) Schmidt, M.; Block, H. D. *Chem. Ber.* **1970**, *103*, 3348–3349.

(30) Wu, R.; Hernández, C.; Odum, J. D.; Dunlap, R. B.; Silks, L. A. *Chem. Commun.* **1996**, 1125–1126.

(31) Ueyama, N.; Okamura, T.; Yamada, Y.; Nakamura, A. *J. Org. Chem.* **1995**, *60*, 4893–4899.

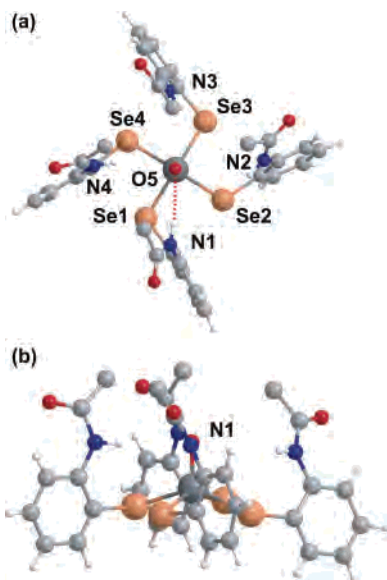


Figure 6. Ball-and-stick representation of the anion part of **3b**, (a) top and (b) side views, where methyl protons are omitted. An intramolecular $\text{NH}\cdots\text{O}=\text{Mo}$ hydrogen bond is shown as a red dotted line.

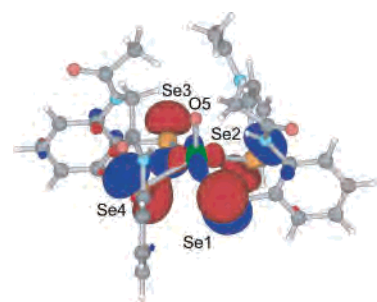


Figure 7. Visual representation of HOMO for $[\text{Mo}^{\text{IV}}\text{O}(\text{Se}-2\text{-CH}_3\text{-CONHC}_6\text{H}_4)_4]^{2-}$.

terminal $\text{O}=\text{Mo}$ have been pointed out in the active sites of native molybdenum enzymes^{32,33} and the model compounds.^{34,35}

Ab initio MO calculations for **3b** were performed to confirm the presence of the $\text{NH}\cdots\text{Se}$ and $\text{NH}\cdots\text{O}=\text{Mo}$ hydrogen bonds on the basis of the crystal structure. Figure 7 shows HOMO of the anion part of **3b**. The MO is located mainly at the MoSe_4 core with antibonding (and nonbonding) $p\pi-d\pi$ interaction, which is essentially the same as that of the reported thiolate analogue.⁸ The MO contains d_{xy} and $d_{x^2-y^2}$ orbitals of molybdenum and p_x (or p_y) and p_z orbitals of selenium. The $p\pi$ orbital, which is directed to the proton of the amide group, is perpendicular to the $\text{Mo}-\text{Se}-\text{C}$ plane and interacts with the $d\pi$ orbital of molybdenum. The $\text{NH}\cdots\text{Se}$ hydrogen bond stabilizes the $\text{Mo}-\text{Se}$ bond by decreasing the antibonding character of the $\text{Mo}-\text{Se}$ bond. Each amide NH group is directed toward the individual

Table 3. Intramolecular $\text{NH}\cdots\text{Se}$ and $\text{NH}\cdots\text{O}=\text{Mo}$ Hydrogen Bonds in the Crystal of **3b**

N-H \cdots A		X-ray ^a		calculated bond order ^b
N-H	A	N \cdots A	H \cdots A	H \cdots A
N1-H1	Se1	3.094(8)	2.865	-0.0012
	O5	3.28(1)	2.399	0.0314
N2-H2	Se2	3.142(8)	2.650	0.0315
	O5	3.822(9)	3.200	0.0003
N3-H3	Se3	3.114(7)	2.562	0.0292
	O5	3.35(1)	2.638	0.0132
N4-H4	Se4	3.120(8)	2.685	0.0124
	O5	3.51(1)	2.658	0.0175

^a H atoms are at calculated positions. ^b Calculated by Gaussian03²² and BORDER.²³

position. To estimate the bond character or strength, bond order was evaluated for the $\text{NH}\cdots\text{O}=\text{C}$ and $\text{NH}\cdots\text{Se}$ hydrogen bonds, where the riding model of SHELXL-97 was used to calculate the positions of the hydrogen atoms.²¹ The bond orders as well as the interatomic distances in the crystal structures are summarized in Table 3. Obviously, only N1 is directed to $\text{O}=\text{Mo}$ with short contact (2.399 Å), with and without attractive $\text{NH}\cdots\text{Se}$ interaction. The bond order was a negative value (-0.0012) for $\text{N1H1}\cdots\text{Se1}$ and a large positive value (0.0314) for $\text{N1H1}\cdots\text{O5}=\text{Mo}$. In comparison, N2H2 formed predominantly $\text{NH}\cdots\text{Se}$ hydrogen bonds. The other NH groups formed both $\text{NH}\cdots\text{Se}$ and $\text{NH}\cdots\text{O}=\text{Mo}$ hydrogen bonds.

Conclusions

The presence of $\text{NH}\cdots\text{Se}$ hydrogen bonds in the monooxomolybdenum(IV) selenolate complex was established by X-ray analysis and by IR and NMR measurements. The $^{77}\text{Se}-^1\text{H}$ COSY strongly supported the presence of $\text{NH}\cdots\text{Se}$ hydrogen bonds with covalent character. Replacing the sulfur atom with selenium successfully produced isostructural compounds and resulted in analogous spectral and electrochemical properties. Using the ^{77}Se NMR technique presented us with indisputable evidence of the existence of intramolecular $\text{NH}\cdots\text{Se}$ and $\text{NH}\cdots\text{S}$ hydrogen bonds. The similarities between cysteine and selenocysteine in terms of their structural and chemical properties suggest that the $\text{NH}\cdots\text{Se}$ hydrogen bond makes significant contributions and possesses biological importance, as has been widely reported for $\text{NH}\cdots\text{S}$ hydrogen bonds in various enzymes.

Acknowledgment. This work was supported by the Grant-in-Aid from the Ministry of Education, Culture, Sports, Science, and Technology, Japan.

Supporting Information Available: X-ray crystallographic data for **3b** and **4** in CIF format, geometrical parameters (Table S1), X-ray structure and calculated bond order of **4** (Figure S1), ^1H NMR spectra (Figure S2) and absorption spectra (Figure S3) of **2a**, IR spectra of **1b** and **2a** (Figure S4), cyclic voltammograms of **1b** and the related compound (Figure S5), ^{77}Se NMR and $^{77}\text{Se}-^1\text{H}$ COSY spectra of the Hg complex (Figure S6). This material is available free of charge via the Internet at <http://pubs.acs.org>.

IC061140Y

(32) Schindelin, H.; Kisker, K.; Hilton, J.; Rajagopalan, K. V.; Rees, D. C. *Science* **1996**, *272*, 1615-1621.

(33) Kisker, K.; Schindelin, H.; Pacheco, A.; Wehbi, W. A.; Garrett, R. M.; Rajagopalan, K. V.; Enemark, J. H.; Rees, D. C. *Cell* **1997**, *91*, 973-983.

(34) Davies, E. S.; Beddoes, R. L.; Collison, D.; Dinsmore, A.; Docrat, A.; Joule, J. A.; Wilson, C. R.; Garner, C. D. *J. Chem. Soc., Dalton Trans.* **1997**, 3985-3995.

(35) Cooney, J. J. A.; Carducci, M. D.; McElhaney, A. E.; Selby, H. D.; Enemark, J. H. *Inorg. Chem.* **2002**, *41*, 7086-7093.